Supporting Information Appendix (SI Appendix)

Supplementary Materials and Methods

Ethics statement. Non-obese diabetic/severe combined immuno deficient (NOD/LtSz-*scid/IL2Rγ*^{null}) (referred to as NSG) mice were p purchased from the Jackson Laboratory (Bar Harbor, ME) (1, 2). Newborn progenies for transplantation experiments were obtained from inbred breeding and maintained under Specific-Pathogen-Free (SPF) conditions. Animal protocols for this study (No. 20100210001) were reviewed and approved by the Institutional Animal Care and Use Committee (IACUC) of Samsung Biomedical Research Institute (SBRI). SBRI is an Association for Assessment and Accreditation of Laboratory Animal Care International (AAALAC) accredited facility. Experiments abided by the Institute of Laboratory Animal Resources (ILAR) guide and were approved by the Institutional Animal Care and Use Committee of SBRI. Human cord blood and fetal liver (hFL) were obtained at Department of Obstetrics and Gynecology, Samsung Medical Center (SMC). Informed, written consent was acquired from the parents of the 3 independent donors. Human protocol for experiments with human materials was approved by the Institutional Review Boards of SMC (IRB File No. 2010-08-159).

Cell preparation for engraftment Human mononuclear cells (hMNC) were isolated from human cord blood using Ficoll-Hypaque density gradient centrifugation. Human (h) hCD34^{+} HSCs were purified by positive selection using the MACS human CD34 MicroBead Kit and autoMACS™ Cell Separator (Miltenyi Biotech, Bergisch Gladbach, Germany). The purity of cord blood hCD34^{+} HSCs was evaluated by flow cytometry analysis using antibodies specific for hLin (BD Biosciences, San Jose, CA), hCD34 (BD), and hCD38 (eBioscience, San Diego, CA) molecules. hLin^{-}/CD34^{+}/CD38^{+} HSC with over 95% purity were used in subsequent studies. For hFL, within 24 hours after an abortion, hFL was sectioned and MSCs (hFL-MSC) were obtained by disintegration of fetal liver using a 70μm mesh (BD). hFL-MSCs were suspended in α-modified Eagle's medium (α-MEM). After 3 to 7 passages, hFL-MSCs were transduced with Lenti viruses that expressed DLK1. The cells were then selected with G418 at 600μg/ml. *DLK1* gene was PCR-amplified from AFT024 cell line (ATCC SCRC-1007™) by using DLK1 primers as follows: forward 5´-GGGTCCATGA CCGCGACCGA AGCC-3´, reverse 5´-CCTAGGTTAG ATCTCCTCGT CGCC-3´.

Induction, purification and concentration and quantification of infectious EBV. High titer of infectious EBV B95-8 virion was produced from B95.8/ZHT cells where extra-copy of viral lytic transactivator ZTA protein was in frame fused to 4-hydroxytamoxifen (4HT)-binding, mutant estrogen receptor (ZHT) (3). The near confluent B95-8/ZHT cells were treated with phorbol ester tetradecanoyl phorbol acetate (TPA), a PKC agonist, 20 ng/ml and hydroxyl tamoxifen at 200 nM for 5–7 days (3). Virus was harvested from cell culture supernatant and concentrated as described (3). The relative 50% transforming dose (TD_{50}) was measured by infecting the concentrated EBV into PBMCs as described (4). Alternatively, the genome copy equivalents were determined by real time qPCR using DNA from 1 x 10^{6} RAJI cells (equivalent to 5 x 10^{6} EBV copies). RAJI cells carry an average of 50 copies of latent viral genomes per cell (5). To infect hNSG with EBV, hNSG mice received HSC for 8 weeks (referred to as ^{8w}hN) or 15 weeks (^{15w}hN), PBS control, or 100 μl EBV

concentrate (equivalent to 2.6 x 10^6 RAJI EBV copy, however also equivalent to approximately 1.5 x 10^3 TD_{50} of B95.8 EBV virus solution) was injected through the tail vein into ^{8w}hN or ^{15w}hN mice. hNSG mice challenged with EBV are referred to as hN-EBV.

Characterization of hNSG mice. Components of HIS in reconstituted mice were analyzed from PBMCs weekly after EBV challenge by flow cytometry. RBC-free PBMCs were stained with monoclonal antibodies specific for hCD3 (UCHT1), hCD8a (OKT8), hCD45RO (UCHL1), hCD19 (HIB19), hCD45 (HI30), hCD45RA (HI100), hCD4 (OKT4) (eBioscience). Stained cells were analyzed on FACSAria (BD Biosciences). Serum and plasma layers were kept at −80℃ for analyses when necessary. DNA was prepared from PBMCs and sera. Infection with EBV in hNSG was verified by conventional or real time qPCR for EBNA1 and GAPDH using primer reported primer sets(6); EBNA-1 primers (F: 5′-GAGGA TCCGC GCGGA AAG-3′, R: 5′-GAGGA TCCGC GCCAA AG-3′).

For mRNA expression, total RNA was isolated using RNeasy mini kit (Qiagen). One microgram of RNA was subjected to reverse transcription using *AccuPower®* RT PreMix (Bioneer) (Daejon, Korea) and PCR using the following primer sets of EBNA1 (F 5'- CCGCA GATGA CCCAG GAGAA, R 5'- TGGAA ACCAG GGAGG CAAAT -3'), EBNA2A (F 5'-CATAG AAGAA GAAGA GGATG, R 5'- GTAGG GATTC GAGGG AATTA), EBNA3C (F 5'-AGAAG GGGAG CGTGT GTTGT, R 5'- GGCTC GTTTT TGACG TCGGC), LMP1 (F 5'- GTACG GGTAC AGATT TCC, R 5'- CTGCC GCCAA CGACC TC), hBCL2 (F 5'- GGCAA ATGAC CAGCA GA, R 5'- TGGCA GGATA GCAGC AC), hCD30 (F 5'- GGTTG AGGCA GCAAA CAGAT GG, R 5'- GAGAT GAGTG ACTTG ATCCT GG) and GAPDH(F 5'-TGCAC CACCA ACTGC TTACC, R 5'-GGCAT GGACT GTCGT CATGA G).

Histopathological *in situ* staining. Spleen sections were stained with hematoxylin & eosin (H&E) or antibodies. Antibody includes mouse monoclonal antibody specific for hCD3 (clone UCHT1), hCD15 (ab53997, Abcam), hBCL2 (226R-14, Cell marque), hIg J chain (FL-137, Santa Cruz), hKi67 (227m-94, Cell marque), hCD20 (clone H1, BD Pharmingen) and hCD3 (F7.2.38, Santa Cruz), hCD30 (Ber-H2, DAKO), hCD68 (EBM11, DAKO), and rabbit polyclonal antibody specific for hCD30 (EPR4102, Abcam) for double staining and phospho tyrosine 461 of STAT6 (NOVUS NB100-2138). Antibody to EBV viral antigen includes mouse monoclonal antibodies to EBNA-1 (clone OT1X, a gift from Dr. Middeldorp, VU University Medical Center, Amsterdam, Netherlands) (clone 0211 (6F9/60), NOVUS NB100-66642), LMP1 (CS1-4) (DAKO) and rat monoclonal antibody to EBNA2 (R3, (Millipore #MABE8). The EBER *in situ* hybridization (ISH) was performed by using the Bond EBER ISH Probe according to manufacturer's instruction (Leica Microsystems, Buffalo Grove, IL, Cat. # PB0589). Sequential double staining for hCD30 (or hCD20)/EBNA1 and hCD30/EBER were performed as described (7).

Statistical analyses. Statistical analyses were performed using GraphPad Prism v.6.0 (GraphPad Software, San Diego, CA). Data are presented as means of experimental measurements and standard errors of the means (SEM). The $P < 0.05$ was considered statistically significant.

Supplementary Results and Discussion

Immune cell repopulation. As consistent with the early appearance of B cell lineage with delayed T cell repopulation in the previous reports (8) (4, 7), the 8-week-reconstitution resulted in B-cell predominance over T cells in almost all mice (12/13 ^{8w}hN mice). Given that human hematopoietic cell repopulation has been known to be observed as early as 6 weeks after CB hCD34^{+} HSC engraftment (8), the predominant B cells in ^{8w}hN in this study would be mostly immature B cells. The B cells was steadily declined thereafter and rapidly shifted to T cell dominance in the following 5 weeks as also described previously(8) (4, 7). In contrast, the 15-week-reconstitution (^{15w}hN) resulted in T-cell predominance in most mice (12/15 ^{15w}hN mice) while the remaining 3 mice showed B-cell dominance (3/15 mice) (Fig. 1; Table 1; Table S1). Taken ^{8w}hN and ^{15w}hN groups together, while predominance of T cells in altogether 16 mice was unaffected until 5 weeks post transplantation (wpt), 13 out of 18 mice with B cell predominance switched to T cell dominance. The B cell dominance in the remaining 5 mice was likely due to B cell expansion as a result of EBV infection (Table 1; Table S1). The above profiles within error ranges were noted until 13 wpt in ^{15w}hN but not in ^{8w}hN (Fig. S1). The 8-week reconstitution resulted in repopulation of hCD45^{+} cells as much as ~5% of total peripheral blood lymphocytes in humanized mice. They are comprised of the vast majority (78%) of presumably immature hCD19^{+} B cells and rare T cells (~2%). Longer reconstitution was needed to repopulate human HSC at the proper level; the 15-week reconstitution substantially increased repopulated efficiency by 3 fold compared to the 8-week condition (hCD45^{+} cells comprised ~15%) and resulted in balanced repopulation between B and T cells (hCD19^{+} B 16%, hCD3^{+} T 65% among hCD45^{+} human lymphocytes) . Lack of activated T cells may be linked to predisposition to NHL in ^{8w}hN following EBV infection. In contrast, abundant T cells in ^{15w}hN can limit an EBV-infected cell proliferation, leaving rare numbers of EBV-infected cells (i.e., Hodgkin-like cells and/or Reed Sternberg (HRS)-like cells) that could have escaped from host immune surveillance.

EBV latency. In contrast to general belief, EBV infection in B cell predominant mice before T cell expansion did not result in type III or EBNA2 expression. B-cell predominant most mice infected with EBV after 8-week reconstitution prior to T-cell expansion (^{8w}hN-EBV), showed type I latency (lack of EBNA2 and LMP1 expression (8 /9 mice as evidenced by IHC and PCR)) (see experimental trial 1). In sharp contrast, mice infected with EBV after 15 weeks of reconstitution (^{15w}hN-EBV) showed both type II (n=6) and III (n=6) at equal frequency, which was followed by rare type I latency (n=1), suggesting that EBV infection at early phase of hematopoiesis may limit expression of certain latent genes and preexisting or developing T cells in this experimental setting may not (or less) properly function (Table S1; Fig. S13).

EBV load in sera. EBV DNA was detected in sera of infected mice as early as 2~3 wpi. Ten-thousand–fold higher titers of EBV particles were detected in hNSG^{15w}-EBV than hNSG^{8w}-EBV mice or injected EBV copy number (2 x 10^{6}). The extremely high level of detected EBV in sera is likely produced from productive infection, which was consistent with an earlier report describing that EBV initially replicates lytically to produce abundant virus particles, then enters a latent state to remain within the host indefinitely(9). Sera of EBV-NHL bearing mice had ~2 fold more maximum level of

viral load than those of EBV-HL-like mice from Exp 2 and Exp 3 settings that essentially adopted the same reconstitution periods (15 weeks) (Fig. 3).

EBVaNHL-like tumors. Both diffuse and nodular (or follicular) proliferation of atypical immunoblast-like lymphocytes in EBVaNHL that replace the normal architecture of lymphoid tissue, were observed in the present study. These cells formed aggregates resembling lymphoid follicles but without germinal centers (SI Appendix, Figure S5 A, left). There was also diffuse distribution of proliferating cells with no clear evidence of follicular aggregation (SI Appendix, Fig. S5 A, right). These atypical lymphocytes were larger (5–7 μm in diameter) than normal lymphocytes (3–4 μm in diameter) and displayed histology characteristic of NHL including vesicular nuclei, prominent nucleoli, and usually basophilic cytoplasm. Overall, the histological features of these cells were highly consistent with human NHL. This suggestion was further supported by immunostaining (See the malignant, abundant hCD20+/hBCL2+ B cells in Fig. 4).

EBVaHL-like tumors in abnormal T cell dominant condition. In low powered view, microscopic architecture of spleen was extensively distorted so that normal lymphoid function units including PALS (periarterial lymphoid sheath) and lymphoid follicle (LF) were extensively effaced. Instead, the normal microscopic structure was replaced by haphazard lymphoid cell proliferation without evident functional structure. The extent of effacement seen in this study was something that can be observed only in malignant condition, not in reactive hyperplasia with mild distortion of lymphoid architecture and enlarged lymphoid follicle.
In high powered view, most of lymphoid cells comprising this lesion appeared to be normal without any morphological features of suggestive malignancies such as enlarged nucleus, irregular chromatin distribution, angular nuclear membrane and prominent nucleolus. However, many cells having morphological features of HRS-like cells were scattered among normal-looking lymphocytes. These HRS-like cells displayed a very prominent nucleoli, highly thickened and irregular nuclear membrane, vesicular chromatin distribution, remarkably enlarged nucleus (Fig. S3, Fig. S4). All of these features suggest that these cells have all pathologic attributes of HRS cells.

Contrasting to the fact that human epithelial microenvironment is necessary for proper self MHC-restricted T cell development in thymus, this humanized mice system only carried human hematopoietic cells but not human thymic epithelial cells and thymic T cells, indicating that human T cells in this humanized mice must be educated in the context of mouse MHC restriction. Therefore, T cells should be suboptimal in controlling cellular immune response against infection. In this regard, we have established new generation of humanized mice which were engrafted with all the necessary microenvironment and hematopoietic stem cells: human thymic, bone tissues and autologous $hCD34^+$ stem cells. A well-conditioned human B and T cell response with an excellent adaptive immune response to T dependent antigens in such novel humanized mice may help to elucidate the role of T cells in controlling acute EBV-induced IM or HL-like tumors (10).

Fewer EBER+ cell than EBNA1+ cells. The odd results of apparently fewer number of EBER positive cells than EBNA1-positive cells were confirmed by additional

staining of consecutive tissue slices from two infected specimens (IF6, IF7) and RAJI cells were performed. The proportion of EBER RNAs *in situ*-positive cells was smaller than that of EBNA1 IHC–positive (EBER 50~60% vs. 80~90% EBNA1 in RAJI, 5~10% vs. 10~30% in spleen of EBVaNHL humanized mice in this revision and Fig S8, S9) (SI Appendix, Fig. S15). Given EBERs are transcribed to high abundance by host RNA polymerase III (POL III)(11, 12) the lower number of EBER+ cells than that of EBNA1+ cells suggested that POLIII-dependent EBER promoter usage is cell cycle-dependent. In fact, several reports already have shown that POL III activity is negatively regulated by RB tumor suppressor during G0 and early G1 in cell-cycle dependent manner(13-16). Scott *et al* described that "RB binds and represses the POL III-specific transcription factor TFIIIB during G(0) and early G(1), but this interaction decreases as cells approach S phase. Full induction of POL III coincides with mid- to late G(1) phase, when RB becomes phosphorylated by cyclin D- and E-dependent kinases". In contrast, because EBNA1 is transcribed by alternatively changing one of three EBV promoters (Wp, Cp, Qp)(17-20) and stabilized via its glycine-alanine repeat-mediated inhibition of proteasome activity (21, 22) almost all EBV-infected cells are constitutively positive for EBNA. Collectively, we assume that non-cycling cells may transcribe less EBER than actively propagating cells while maintaining EBNA1 at constitutively level. As for Fig 3D and 4A, please be advised that area (or specimen ID) of EBER *in situ* were different from those of EBNA1 because of usual unavailability of consecutive or failure in staining. In addition, please be advised that similar staining pattern was also seen in a previous EBV humanized mouse (23).

Differential diagnosis of hCD30$^+$ and hCD15$^+$ HRS-like cells from activated B/T cells, macrophages and mature granulocytes. Both hCD30 and hCD15 can be expressed in activated B cells, T cells, macrophages in subsets of DLBCLs. However the diagnosis of HL is made primarily on histology basis. HRS cells have distinct cellular morphology; therefore can be distinguished from activated normal cells such as activated B cells, T cells, and macrophages. For instance, histological hallmarks of HRS cells such as exceedingly enlarged nucleus, aberrant chromatic distribution with extreme vesicular nuclei, and prominent nuclei are not seen in activated lymphocytes and macrophages, strong indicative of malignant cells. Next, a subset of DLBCLs can show some of HRS-related histological features. In this case, differential diagnosis is primarily made by extent of cytological atypism of background lymphocytes. DLBCLs show extensive cytological atypism in background lymphocytes with variable extent of atypsim. Therefore, the gradual transition of highly atypical cancer cells to moderately atypical background lymphocyte is observed. In fact, almost every cell in DLBCLs is tumor cell with variable cytological atypia. However, in HL, there is highly distinct discontinuity in cytological atypism between HRS cells and background lymphocytes. In our HL-like lesions, background lymphocytes appear to be normal without any cytological atypia. Therefore, the possibility of a subset of DLBCL can be excluded in our cases.
The positivity of hCD30, hCD15 and phospho STAT6 in HRS- like cells in our lesion strengthened the diagnosis of Hodgkin's lymphoma. In addition, taking all hCD30/hCD15, EBNA1/EBER, phospho STAT6 and V_H nonsense mutation into consideration together most likely indicates those are EBV-associated HL or HL- like malignant cells (Fig. 4). Limited search of extra-splenic lymphoma found two pancreatic lymphomas (1 in 8 NHL and 1 in 5 HL-like mice examined) (SI Appendix,

Fig. S16). Though dissociated splenocytes from infected mice started to grow, almost all cells stopped growing and died following 2nd~3rd passages (SI Appendix, Fig. S17). It is also possible that the HL-like cells analyzed in this study might be derived from seemingly type III IM cells after germinal center reaction in response to EBV antigen. The role of acute infection in HL development via apparent IM will be a subject of future study using the third generation of humanized mice recently developed by the authors (10). A well-conditioned human B and T cell response with an excellent adaptive immune response to T dependent antigens in such novel humanized mice may help to elucidate the role of T cells in controlling EBV-induced acute lymphoproliferation.

Role of human mesenchymal stem cell (hMSC) and DLK1 in hematopoiesis

Hematopoietic organs-derived MSCs have an immunosuppressive function. MSCs suppress an alloantigen- and mitogen-activated T-cell development and proliferation. MSCs inhibit cytokine secretion (interleukin-12, tumor necrosis factor-α, interferon-γ) from activated T-cells. MSC-mediated suppression of T-cells results in concomitant B-cell dominance (24, 25). In this MSC-mediated suppressed T-cell condition, EBV-infection of B-cells may cause infected cells to over-proliferate, resulting in B cell lymphoma (BCL). Notch signaling governs T cell versus B cell fate decisions and is critical for T cell lineage commitment. Notch signaling promotes development of T cells (26, 27). Constitutive active form of Notch abolishes B cell development whereas it promotes T cell development in mice and in vitro (28). Conditional inactivation of Notch-1 displays a blockage in T cell development with the concomitant development of B cells as a result of inefficient recombination at the TCR-β locus (29, 30).

It is known that, while BM-derived non hematopoietic stromal cells support B cell lymphopoiesis, the same cell line ectopically expressing a notch activating ligand DLK1 induce T cell proliferation and differentiation into CD4 CD8 double- and single-positive T cells with functional T cell receptor (TCR)(31). Very consistently to reported results (24, 25) (28-31), non autologous FL-derived MSC in this study induced the differentiation of B lymphocytes from HSCs. Moreover, MSC ectopically expressing an appropriate Notch ligand, DLK1, redirected HSC differentiation to adopt T cell fate. DLK1 expression in MSCs *in vivo* most likely induces pro-inflammatory cytokines and chemokines that induce a growth of activated T-cells as described (32). Unlike suppressed T-cells, activated T-cells are abundant and likely control proliferation as well as limit EBV-infected B-cells. This control should result in the survival of rare malignant cells that are present in the background of nonmalignant predominant lymphocyte as seen in HL-like tumor. These data suggest that distinct immune cell predominance may associate with certain type of EBV-induced B cell lymphoma.

Supporting References

1. **Ito M*, et al.* (2002) NOD/SCID/gamma(c)(null) mouse: an excellent recipient mouse model for engraftment of human cells. *Blood* 100(9):3175-3182.**
2. **Shultz LD*, et al.* (2005) Human lymphoid and myeloid cell development in NOD/LtSz-scid IL2R gamma null mice engrafted with mobilized human hemopoietic stem cells. *Journal of immunology (Baltimore, Md. : 1950)***

174(10):6477-6489.
3. Johannsen E*, et al.* (2004) Proteins of purified Epstein-Barr virus. *Proc Natl Acad Sci U S A* 101(46):16286-16291.
4. Yajima M*, et al.* (2008) A new humanized mouse model of Epstein-Barr virus infection that reproduces persistent infection, lymphoproliferative disorder, and cell-mediated and humoral immune responses. *The Journal of infectious diseases* 198(5):673-682.
5. Islas-Ohlmayer M*, et al.* (2004) Experimental infection of NOD/SCID mice reconstituted with human CD34+ cells with Epstein-Barr virus. *Journal of virology* 78(24):13891-13900.
6. Jebbink J*, et al.* (2003) Development of real-time PCR assays for the quantitative detection of Epstein-Barr virus and cytomegalovirus, comparison of TaqMan probes, and molecular beacons. *The Journal of molecular diagnostics : JMD* 5(1):15-20.
7. Ma SD*, et al.* (2012) An Epstein-Barr Virus (EBV) mutant with enhanced BZLF1 expression causes lymphomas with abortive lytic EBV infection in a humanized mouse model. *Journal of virology* 86(15):7976-7987.
8. Lang J*, et al.* (2013) Studies of lymphocyte reconstitution in a humanized mouse model reveal a requirement of T cells for human B cell maturation. *Journal of immunology (Baltimore, Md. : 1950)* 190(5):2090-2101.
9. Halder S*, et al.* (2009) Early events associated with infection of Epstein-Barr virus infection of primary B-cells. *PloS one* 4(9):e7214.
10. Chung YS*, et al.* (2015) Co-transplantation of human fetal thymus, bone and CD34 cells into young adult immunodeficient NOD/SCID IL2Rgamma mice optimizes humanized mice that mount adaptive antibody responses. *Clinical immunology (Orlando, Fla.)*.
11. Howe JG & Shu MD (1989) Epstein-Barr virus small RNA (EBER) genes: unique transcription units that combine RNA polymerase II and III promoter elements. *Cell* 57(5):825-834.
12. Minarovits J*, et al.* (1992) RNA polymerase III-transcribed EBER 1 and 2 transcription units are expressed and hypomethylated in the major Epstein-Barr virus-carrying cell types. *The Journal of general virology* 73 (Pt 7):1687-1692.
13. Larminie CG*, et al.* (1997) Mechanistic analysis of RNA polymerase III regulation by the retinoblastoma protein. *The EMBO journal* 16(8):2061-2071.
14. Ernens I*, et al.* (2006) Hypoxic stress suppresses RNA polymerase III recruitment and tRNA gene transcription in cardiomyocytes. *Nucleic acids research* 34(1):286-294.
15. Goodfellow SJ & White RJ (2007) Regulation of RNA polymerase III transcription during mammalian cell growth. *Cell cycle (Georgetown, Tex.)* 6(19):2323-2326.
16. Scott PH*, et al.* (2001) Regulation of RNA polymerase III transcription during cell cycle entry. *The Journal of biological chemistry* 276(2):1005-1014.
17. Nilsson T, Sjoblom A, Masucci MG, & Rymo L (1993) Viral and cellular factors influence the activity of the Epstein-Barr virus BCR2 and BWR1 promoters in cells of different phenotype. *Virology* 193(2):774-785.

18. Taylor KA, Wetzel S, Lyles DS, & Pollok BA (1994) Dual EBNA1 promoter usage by Epstein-Barr virus in human B-cell lines expressing unique intermediate cellular phenotypes. *Journal of virology* 68(10):6421-6431.
19. Tsai CN, Liu ST, & Chang YS (1995) Identification of a novel promoter located within the Bam HI Q region of the Epstein-Barr virus genome for the EBNA 1 gene. *DNA and cell biology* 14(9):767-776.
20. Yoshioka M, Kikuta H, Ishiguro N, Ma X, & Kobayashi K (2003) Unique Epstein-Barr virus (EBV) latent gene expression, EBNA promoter usage and EBNA promoter methylation status in chronic active EBV infection. *The Journal of general virology* 84(Pt 5):1133-1140.
21. Levitskaya J*, et al.* (1995) Inhibition of antigen processing by the internal repeat region of the Epstein-Barr virus nuclear antigen-1. *Nature* 375(6533):685-688.
22. Levitskaya J, Sharipo A, Leonchiks A, Ciechanover A, & Masucci MG (1997) Inhibition of ubiquitin/proteasome-dependent protein degradation by the Gly-Ala repeat domain of the Epstein-Barr virus nuclear antigen 1. *Proceedings of the National Academy of Sciences of the United States of America* 94(23):12616-12621.
23. Ma SD*, et al.* (2011) A new model of Epstein-Barr virus infection reveals an important role for early lytic viral protein expression in the development of lymphomas. *Journal of virology* 85(1):165-177.
24. Plumas J*, et al.* (2005) Mesenchymal stem cells induce apoptosis of activated T cells. *Leukemia* 19(9):1597-1604.
25. Kim N*, et al.* (2013) Mesenchymal stem cells for the treatment and prevention of graft-versus-host disease: experiments and practice. *Annals of hematology* 92(10):1295-1308.
26. Washburn T*, et al.* (1997) Notch activity influences the alphabeta versus gammadelta T cell lineage decision. *Cell* 88(6):833-843.
27. Izon DJ*, et al.* (2001) Notch1 regulates maturation of CD4+ and CD8+ thymocytes by modulating TCR signal strength. *Immunity* 14(3):253-264.
28. Pui JC*, et al.* (1999) Notch1 expression in early lymphopoiesis influences B versus T lineage determination. *Immunity* 11(3):299-308.
29. Radtke F*, et al.* (1999) Deficient T cell fate specification in mice with an induced inactivation of Notch1. *Immunity* 10(5):547-558.
30. Wolfer A, Wilson A, Nemir M, MacDonald HR, & Radtke F (2002) Inactivation of Notch1 impairs VDJbeta rearrangement and allows pre-TCR-independent survival of early alpha beta Lineage Thymocytes. *Immunity* 16(6):869-879.
31. Schmitt TM & Zuniga-Pflucker JC (2002) Induction of T cell development from hematopoietic progenitor cells by delta-like-1 in vitro. *Immunity* 17(6):749-756.
32. Abdallah BM*, et al.* (2007) dlk1/FA1 regulates the function of human bone marrow mesenchymal stem cells by modulating gene expression of pro-inflammatory cytokines and immune response-related factors. *The Journal of biological chemistry* 282(10):7339-7351.

Table S1. Detail of humanized mice according to reconstitution protocols

Exp	#Group	1ID	2Grafted cell	5How long reconstituted (w)	*Profiles after reconstitution at 1d before challenge				9EBV or PBS	**5w after EBV or PBS challenge				10Immune cell evolution	11Malignant Phenotype	12IHC			13Latency
					6hCD45	7hCD19	7hCD3	8Dominance	challenged	6hCD45	7hCD19	7hCD3	8Dom	(B<->T)	(NHL, HL)	EBNA1 OT1x	EBNA2 R3	LMP1 CS1-4	by IHC
		1M1	hCD34+	8	5	69	9	B	PBS	13.6	<1	25.7	T	B->T	-	-	-	-	na
		1M2	hCD34+	8	5	73	<1	B	PBS	15.2	<1	88.7	T	B->T	-	-	nd	nd	na
		1F3	hCD34+	8	3	86	6	B	PBS	20.4	<1	84.7	T	B->T	-	-	nd	nd	na
		1F4	hCD34+	8	7	83	2	B	PBS	10	2.6	85.6	T	B->T	-	-	nd	nd	na
		1M5	hCD34+	8	17	5	36	T	EBV	na	na	na	na	T->T#	-	-/+	nd	nd	na
		1F6	hCD34+	8	6	87	2	B	EBV	5.1	24.3	46.5	T	B->T	NHL	+	-	-	1
1	8whN	1F7	hCD34+	8	13	91	2	B	EBV	13.3	13.4	68.1	T	B->T	NHL	+	nd	-	1
		1F8	hCD34+	8	7	83	2	B	EBV	na	na	na	na	B->T#	NHL	+	nd	-	1
		1F9	hCD34+	8	4	87	1	B	EBV	5.2	3.5	64.6	T	B->T	NHL	+	-	-	1
		1F10	hCD34+	8	4	87	1	B	EBV	5.7	5.7	72	T	B->T	NHL	+	-	-	1
		1F11	hCD34+	8	3	86	1	B	EBV	5.5	4.7	70.5	T	B->T	NHL	+	-	-	1
		1M12	hCD34+	8	9	91	2	B	EBV	1.7	65.8	1.3	B	B->B	NHL	-/+	-	+	2a
		1M13	hCD34+	8	3	85	<1	B	EBV	0.9	20.9	27.9	T~B	B->T	NHL, TCL	+	nd	-	na
		2-1	hCD34+	15	1.4	12.5	62.5	T	PBS	19.5	<1	75	T	T->T	-	-	nd	nd	na
		2-3	hCD34+	15	10.9	9.9	64	T	PBS	23.7	12.6	79.8	T	T->T	-	-	nd	nd	na
		4-1	hCD34+	15	40.1	1.7	75.5	T	PBS	14	<1	66.7	T	T->T	-	-	nd	nd	na
		4-5	hCD34+	15	23	3.8	75.5	T	PBS	NA	ns	ns	na	T->T#	-	-	nd	nd	na
		2-2	hCD34+	15	8.4	1	92.2	T	PBS	10.5	3	85.8	T	T->T	-	-	nd	nd	na
		4-3	hCD34+	15	20.5	4.2	75.9	T	EBV	24.4	3.8	81.6	T	T->T	NHL	+	-	-	1
		3-1	hCD34+	15	0.3	66.7	33.7	B	EBV	0.4	18.8	<1	B	B->B	NHL	+	+	+	3
2	15whN	1-2	hCD34+	15	9.7	14.3	57.1	T	EBV	23.3	2.7	92.5	T	T->T	HL, NHL	-/+	+	+	3
		2-4	hCD34+	15	17.7	6.7	83.3	T	EBV	19.8	6.3	85.1	T	T->T	HL, NHL	+	-/+	+	2a
		4-4	hCD34+	15	25.6	18.2	45.5	T	EBV	6.5	25	41.7	T	T->T	HL	-/+	-	+	2a
		1-4	hCD34+	15	12.5	4.8	88.1	T	EBV	38.5	11.9	74.4	T	T->T	HL	-/+	-	+	2a
		3-2	hCD34+	15	9.8	<1	91.7	T	EBV	33.4	<1	95.7	T	T->T	HL	+	-	+	2a
		1-3	hCD34+	15	32.1	2.1	63	T	EBV	8	9.9	76.1	T	T->T	-	-	nd	nd	na
		1-1	hCD34+	15	3.5	59.5	13.6	B	EBV	34.2	31.7	39	T~B	B->T	-	-	nd	nd	na
		4-2	hCD34+	15	1.6	27.3	<1	B	EBV	0.2	9.1	<1	B	B->B	-	-	nd	nd	na
		5-1	34+/MSC3	15	4.1	20	<1	B	EBV	8.3	37.5	<1	B	B->B	-	-/+	nd	nd	na
		5-3	34+/MSC	15	1.1	38.9	5.6	B	EBV	2.8	52	<1	B	B->B	NHL	+	+	+	3
3	15whNMSC	2M2	34+/MSC	15	45	59	21.1	B	EBV	7.3	15	52.1	T	B->T	NHL	+	nd	+	2a/3
		6-1	34+/M DLK14	15	15	<1	66.7	T	EBV	12.3	5.2	79.9	T	T->T	HL	+	+	+	3
		7-1	34+/M DLK1	15	19.7	8.4	85.3	T	EBV	10.5	<1	95.7	T	T->T	HL	+	+	+	3
		5-2&	34+/M DLK1	15	0.9	1	33.3	T	EBV	2.8	<1	52	T	T->T	HL,NHL	+	-	+	2a

#Group of humanized mice which were given for 8 and 15 weeks, respectively, (8whN or 15whN) for immune cell reconstitution following HSC graft, and 15 weeks after co engraftment with HSC and MSC (15whMSC), *Corresponds at 8 weeks and 15 weeks after graft for Exp 1 and Exp 2~3 respectively, **Corresponds at 13 and 20 weeks after graft for Exp 1 and Exp 2~3 respectively, 1New born NSG at 1 day after the birth, 2hCD34+fetal human cord blood hCD34+ hematopoietic stem cells 2x105, 3Conengraftment of hCD34+ HSC and mesenchymal stem cell (MSC), 4Conengraftment of hCD34+ HSC and MSC expressing notch activator DLK1 gene, 5Weeks given for reconstitution after graft, 6Total human CD45+ leukocytes fraction in mouse PBMC, 7hCD19+ B (hCD3+ T) cells among gated hCD45+, 8Dominant cell type at indicated time points, 9Injection of B95.8 supernatant or PBS though tail vein, 10Evolution of dominant cell type from before and 5 weeks after infection with EBV or PBS, #presumed dominance after considering data from the same conditions, Note the evolution data summarized in Fig. 1 and Table 1. 11Non Hodgkin's types B cell lymphoma (NHL), Hodgkin's lymphoma (HL), or Hyperplasia (HP) at the age of 28~30 weeks, 12Immunohistochemical staining, 13Latency typed by IHC, type 1 (EBNA1/EBER; type 2a, EBNA1/EBER/LMP1; type 2b, EBNA1/EBER/EBNA2; type 3, EBNA1/EBER/LMP1/EBNA2, na not applicable, &from an independent

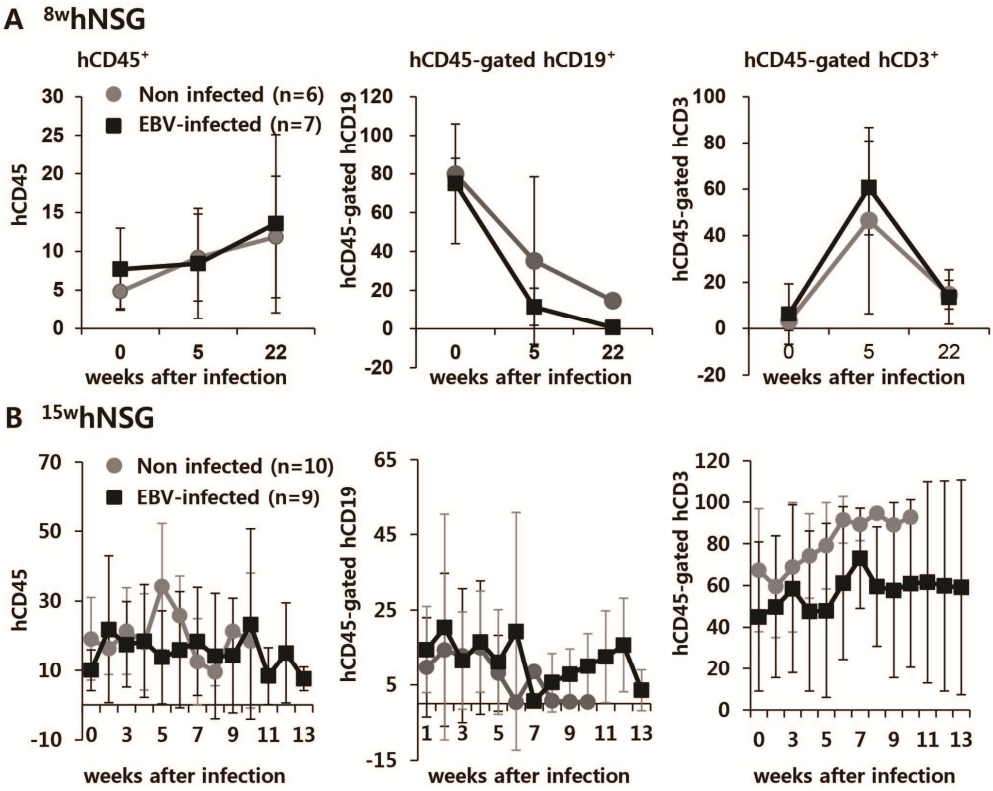

Fig. S1. Human immune cell profile in PBMCs between EBV-noninfected and –humanized mice. **A)** No changes in ^{8w}hN until 22 weeks post-infection (wpi). **B)** Slightly more B with less T cell fraction within error ranges upon EBV infection in ^{15w}hN until 13 wpi. Data points are indicated as mean ± a standard error (SEM).

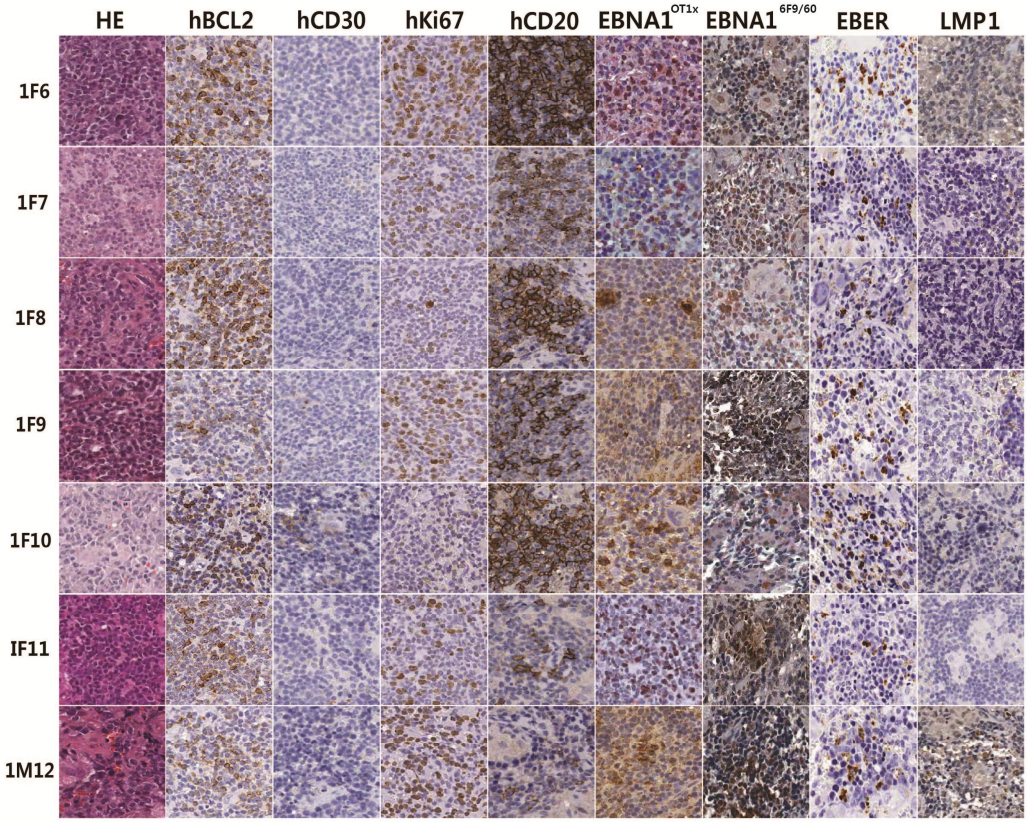

Fig. S2. IHC staining of splenic tissues of ^{8w}hN-EBV mice with NHL. Most NHL tissues showed a positive staining for typical EBVaNHL markers (hBCL2^{+}, hKI67^{+}, hCD20^{+}, EBNA1^{+}, EBER^{+}), but negative staining (EBNA2^{-}, LMP1^{-}) and HL marker (CD30^{-}). The number in the left denotes mouse individual number described in Table S1. Two EBNA1 monoclonal antibodies (OTX1, 6F9/60) were used.

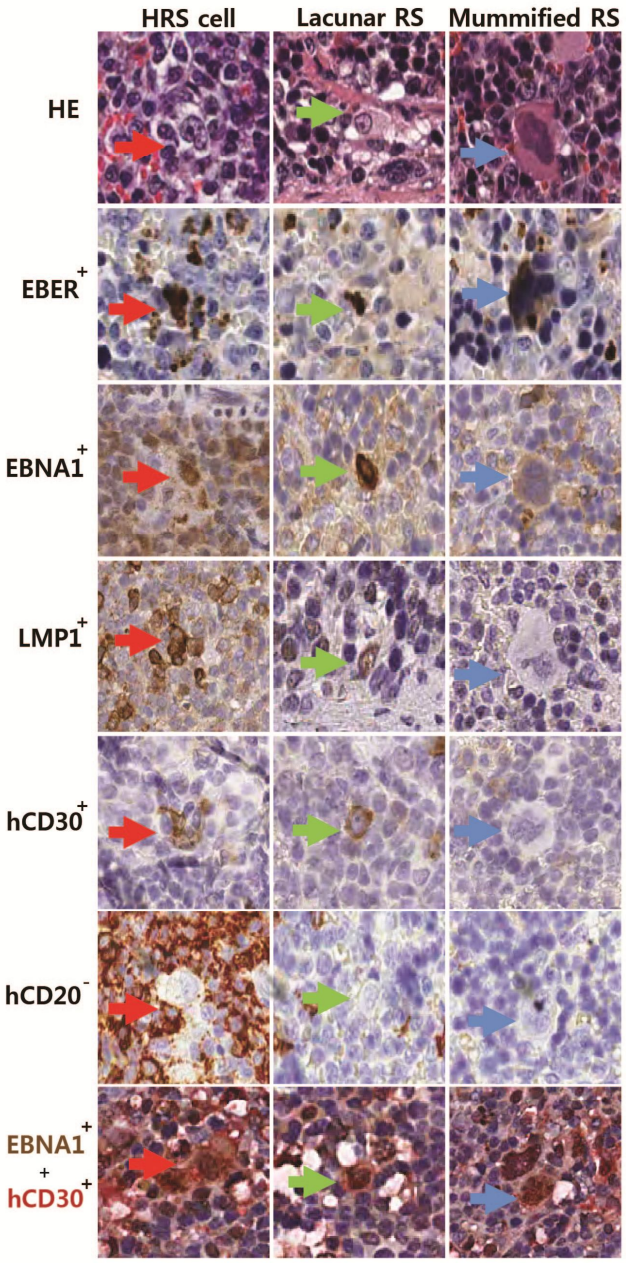

Fig. S3. Expressions of viral and HL markers in spleen of T cell predominant mice with HL-like disorder A) IHC staining. Multiple HRS (red arrow), lacunar typed RS (green arrow), and mummified RS (blue arrow) cells were observed (average 24 cells per spleen of HL). Malignant HRS cells were positive for EBVaHL markers ($EBER^+$, $LMP1^+$, $EBNA1^+$, $EBNA^+/hCD30^+$, $hCD30^+$) but negative NHL markers ($hCD20^-$, $EBNA2^-$) (see $hCD20^-$ malignant RS-like cells (black arrow) in the $hCD20^{-/weak}$ background) . Each color indicates staining of indicated antigens.

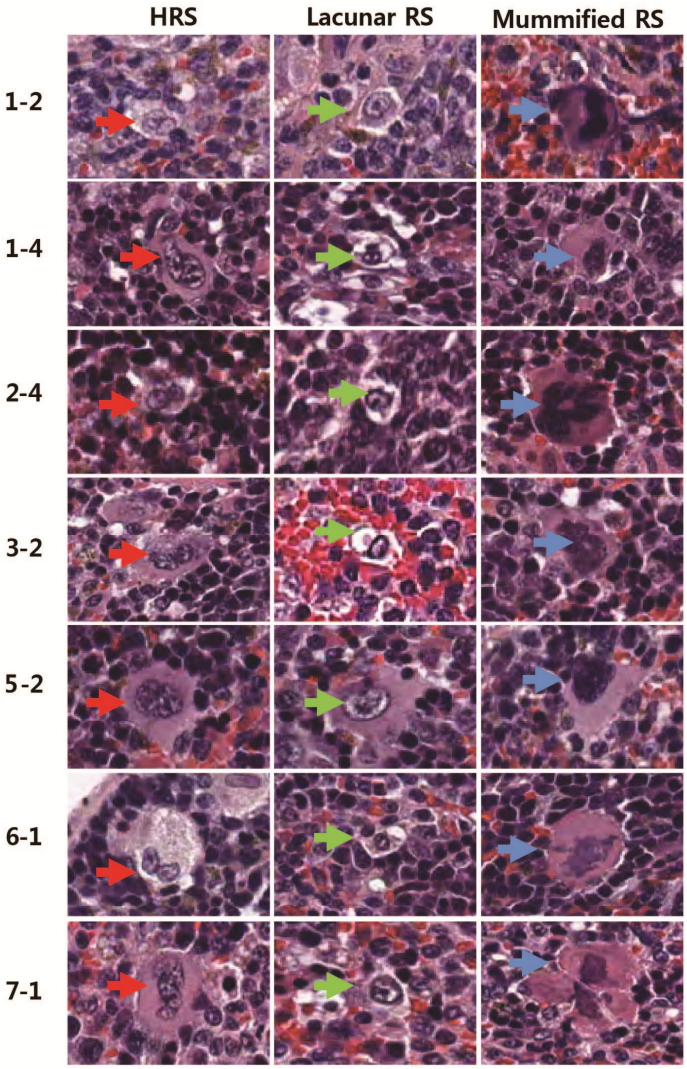

Fig. S4. Additional HRS or RS-like images in all HL-bearing mice. Multiple HRS (red arrow), lacunar typed RS (green arrow), and mummified RS (blue arrow) cells were observed (average 24 cells per spleen of HL). The number in the left denotes mouse individual number described in Table S1.

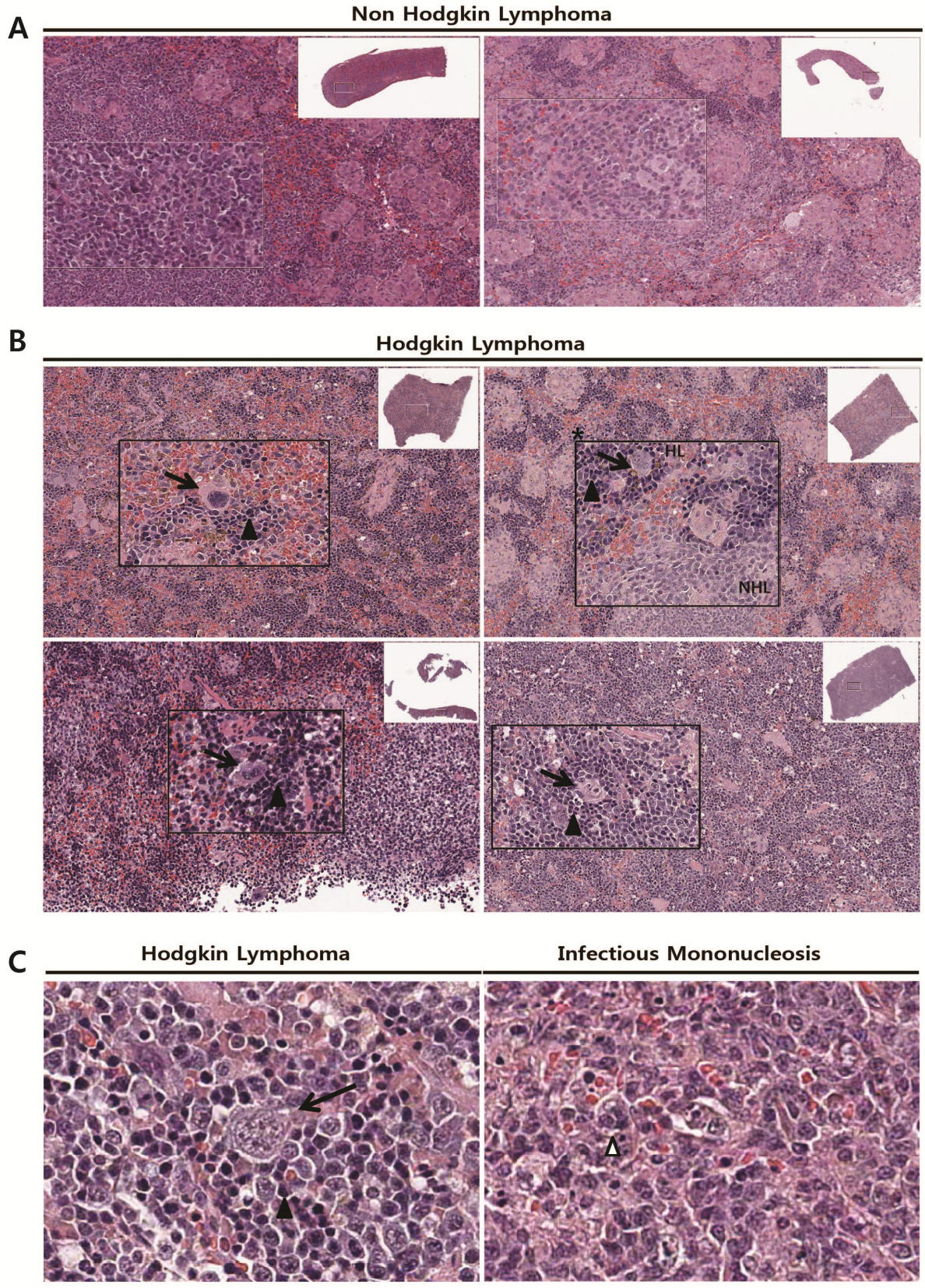

Fig. S5. EBV-associated lymphomas H&E microscope graphs of spleens from humanized mice in this study. **A)** H&E staining of spleen from EBV-infected

humanized mice with NHL. Note proliferation of histiocyte. **B)** H&E staining of spleens from EBV-infected humanized mice with HL-like tumor. Whole spleen was shown on the upper right corner. Closed-up images were embedded on the low-powered image. **C)** Closed up images of H&E of HL (left) and IM (right) in the same humanized mice (ID 4-2) (see Discussion section for detail). In HL, typical HRS cell (arrow) was typically surrounded mostly by normal-looking lymphocytes (filled arrow head). In IM, the rare lymphocytes (filled arrowhead) and HRS-like cells were observed in the admixture of abundant immunoblasts (unfilled arrowhead)

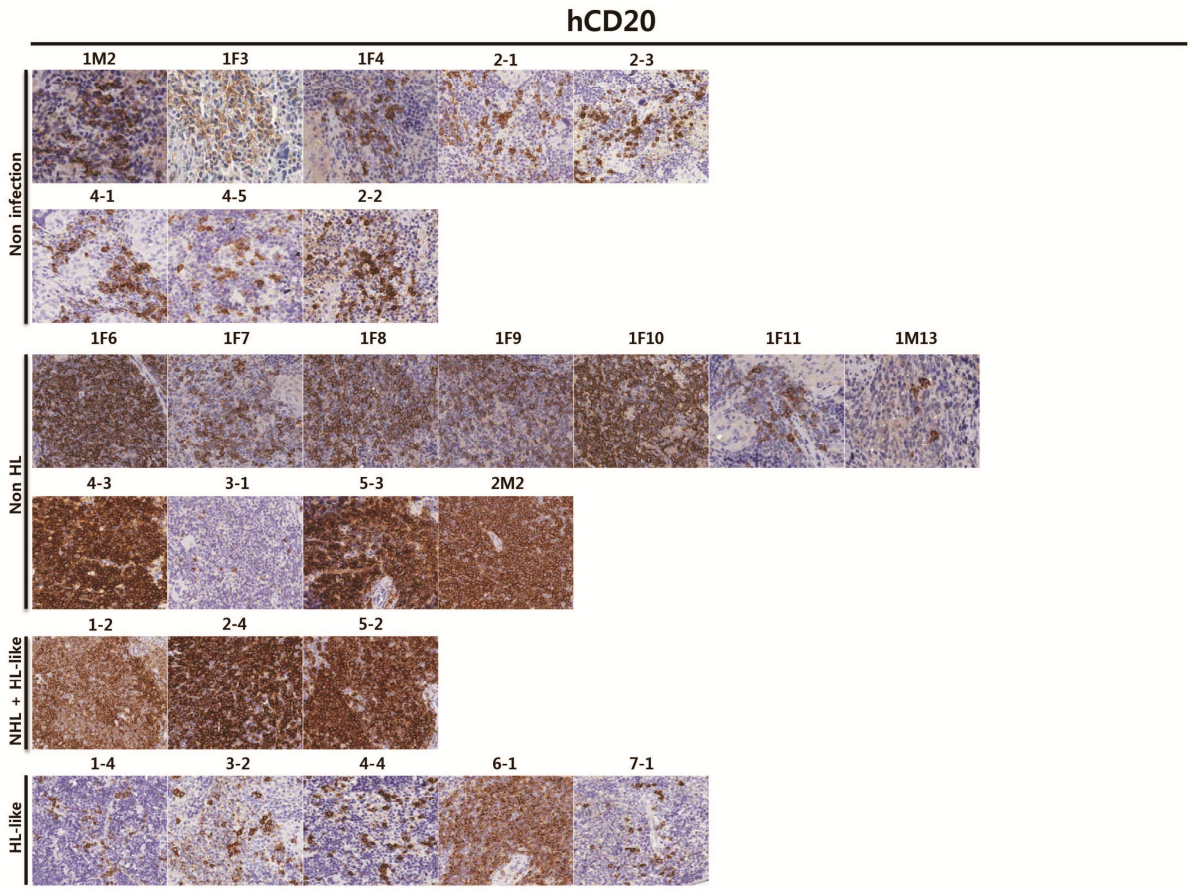

Fig. S6. IHC staining of hCD20 for spleen of humanized mice. Note high abundance in NHL but less or weak abundance in HL tissue, which was consistent with lymphoma criteria of REAL/WHO.

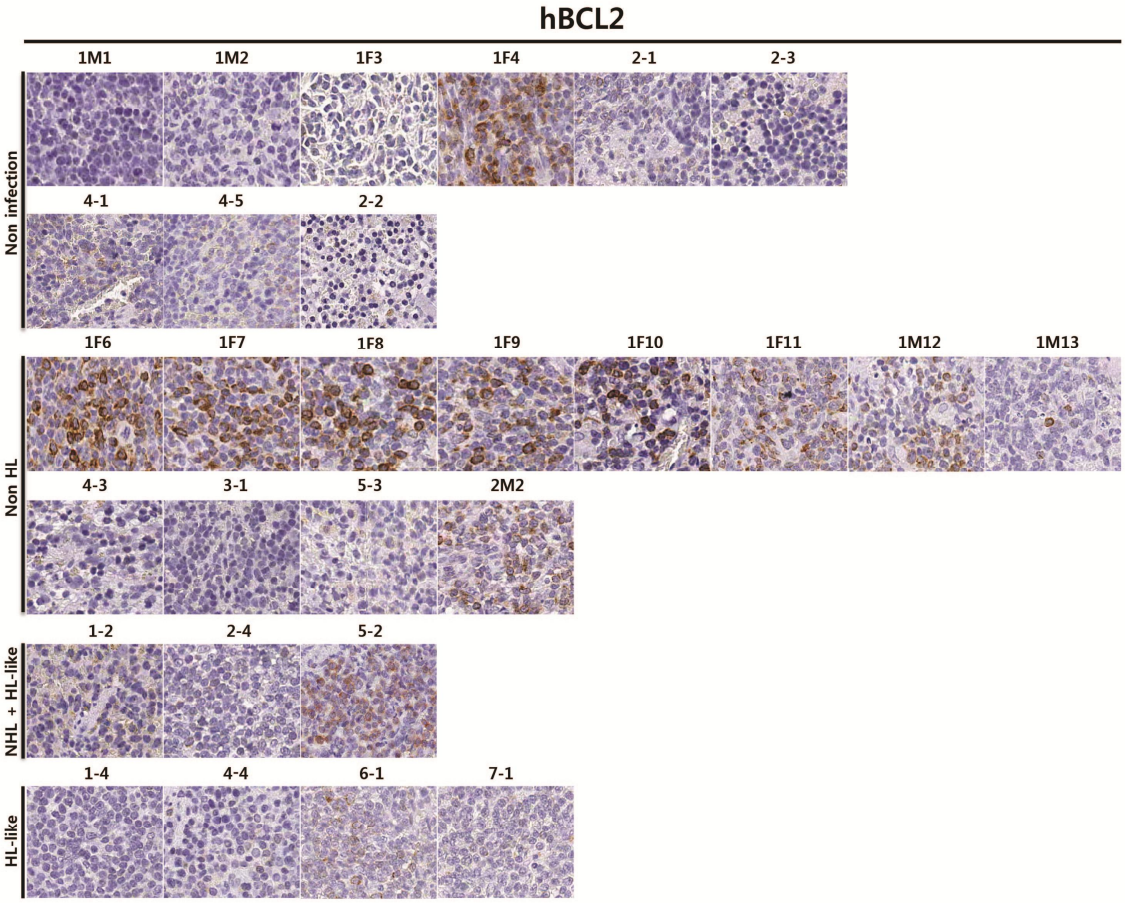

Fig. S7. IHC staining of hBCL2 for spleen of humanized mice

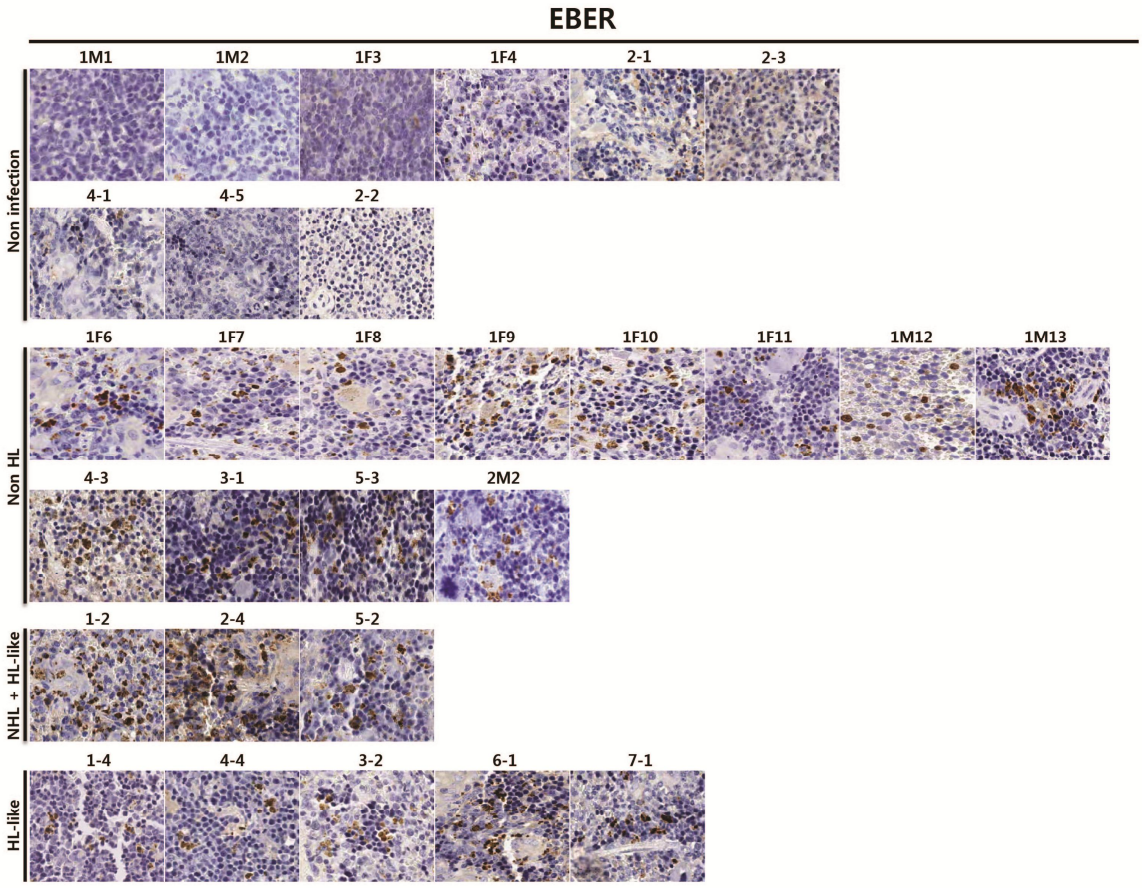

Fig. S8. *In situ* staining of EBER for spleen of humanized mice

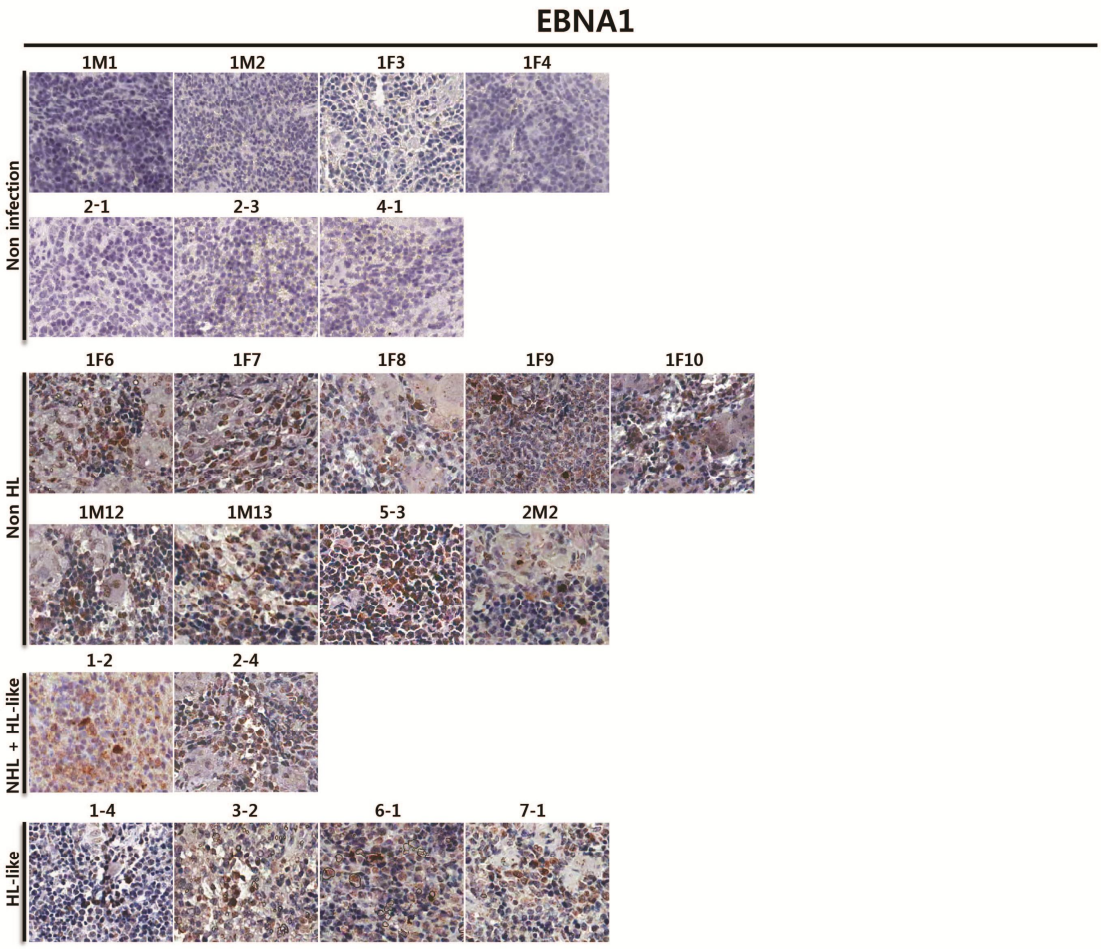

Fig. S9. IHC staining of EBNA1 for spleen of humanized mice

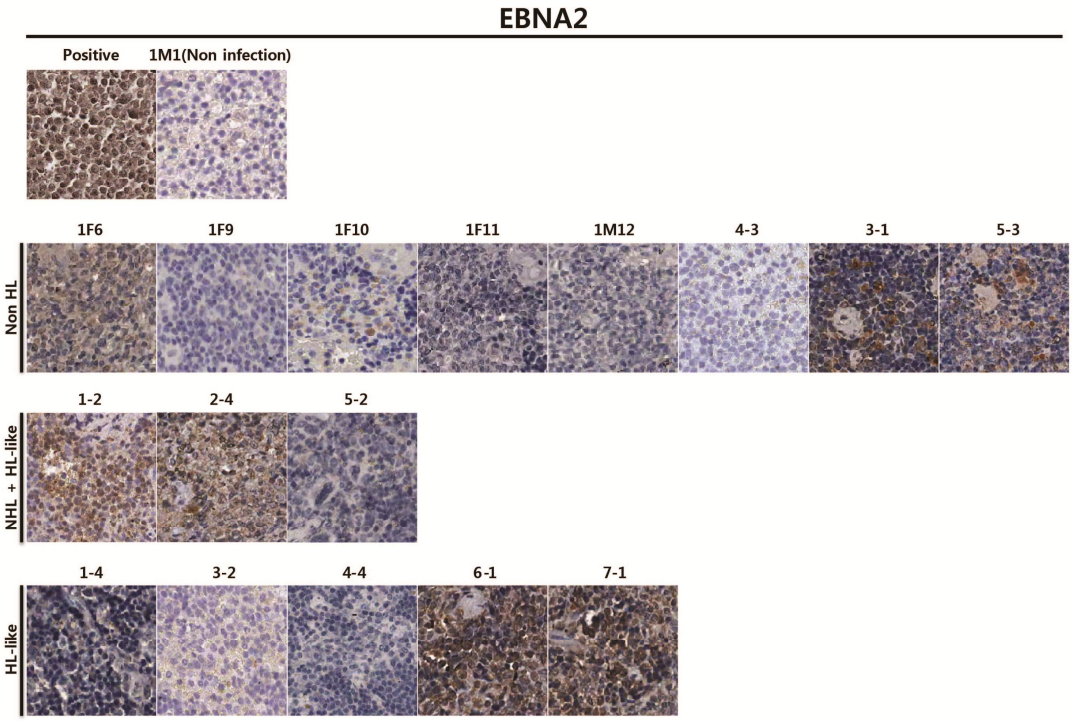

Fig. S10. IHC staining of EBNA2 for spleen of humanized mice

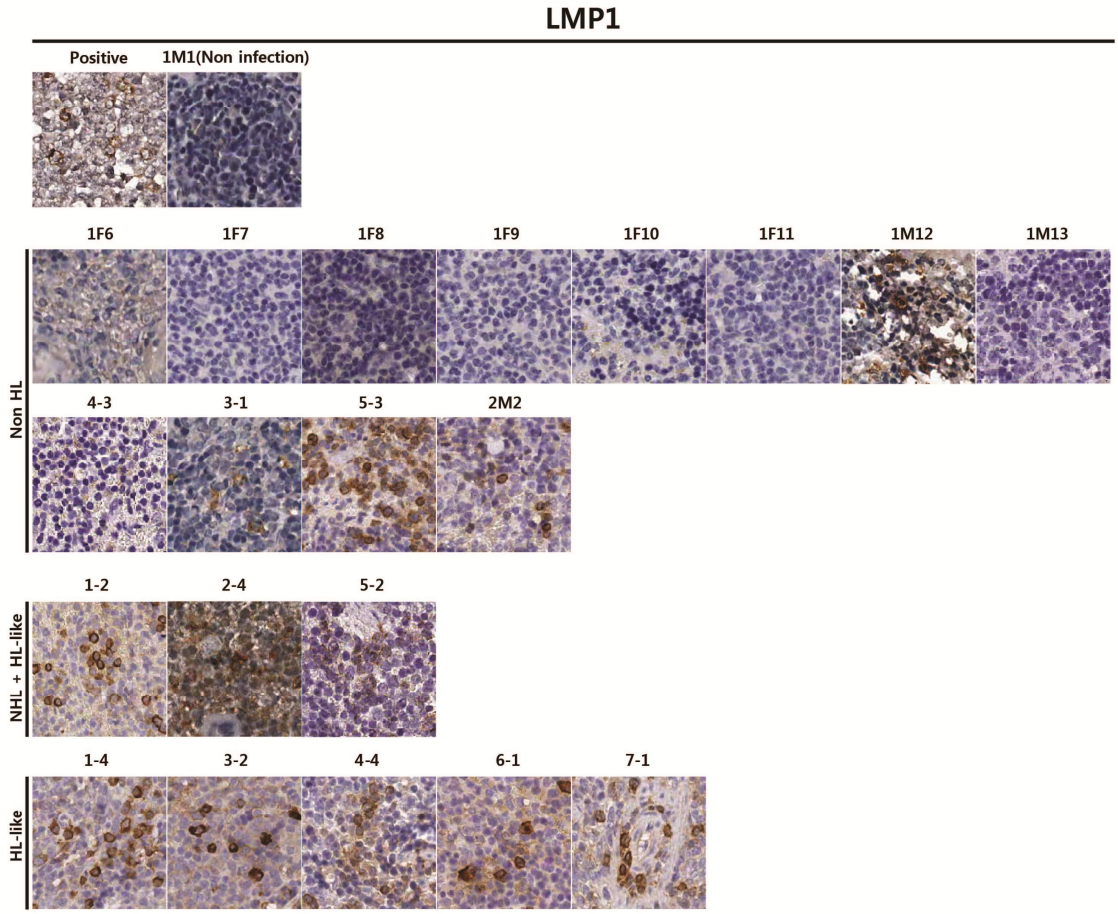

Fig. S11. IHC staining of LMP1 for spleen of humanized mice

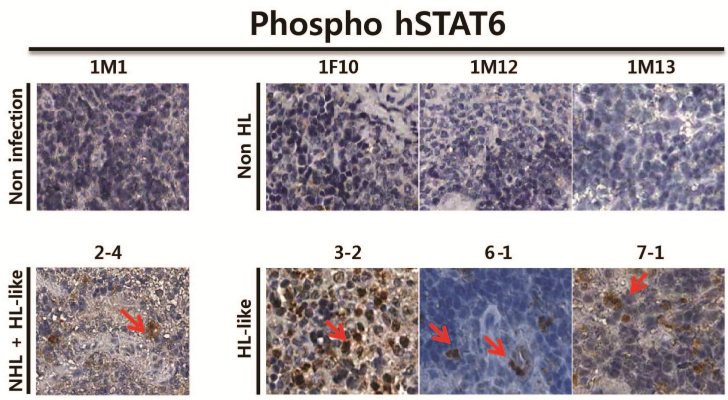

Fig. S12. IHC staining of phospho STAT6 for spleen of humanized mice

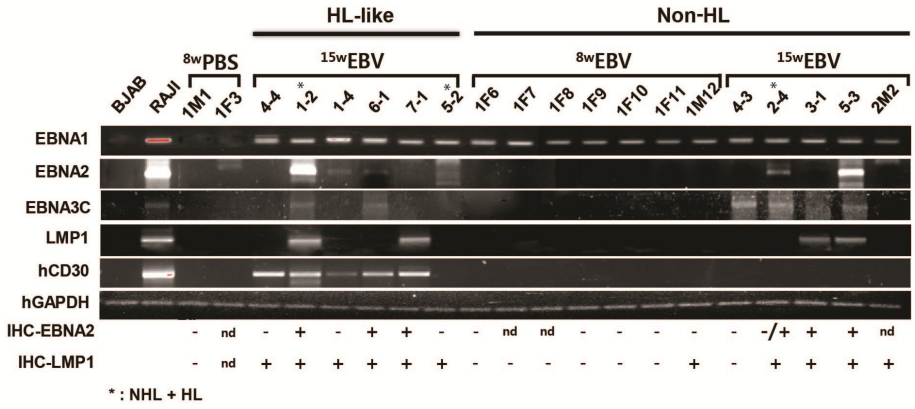

Fig. S13. PCR analyses of mRNA expression in humanized splenocyte. EBV-negative BJAB BL, EBV-infected RAJI type III BL cell lines and PBS-injected humanized mice were used as a negative or positive control. *Note that mouse 2-4 has both NHL and HL-like tumor. RNA isolated from thin slice from a certain depth in paraffin embedded tissue does not necessary represent *in situ* expression pattern than can be seen at the whole spleen level, likely accounting for variation or inconsistency between PCR and IHC.

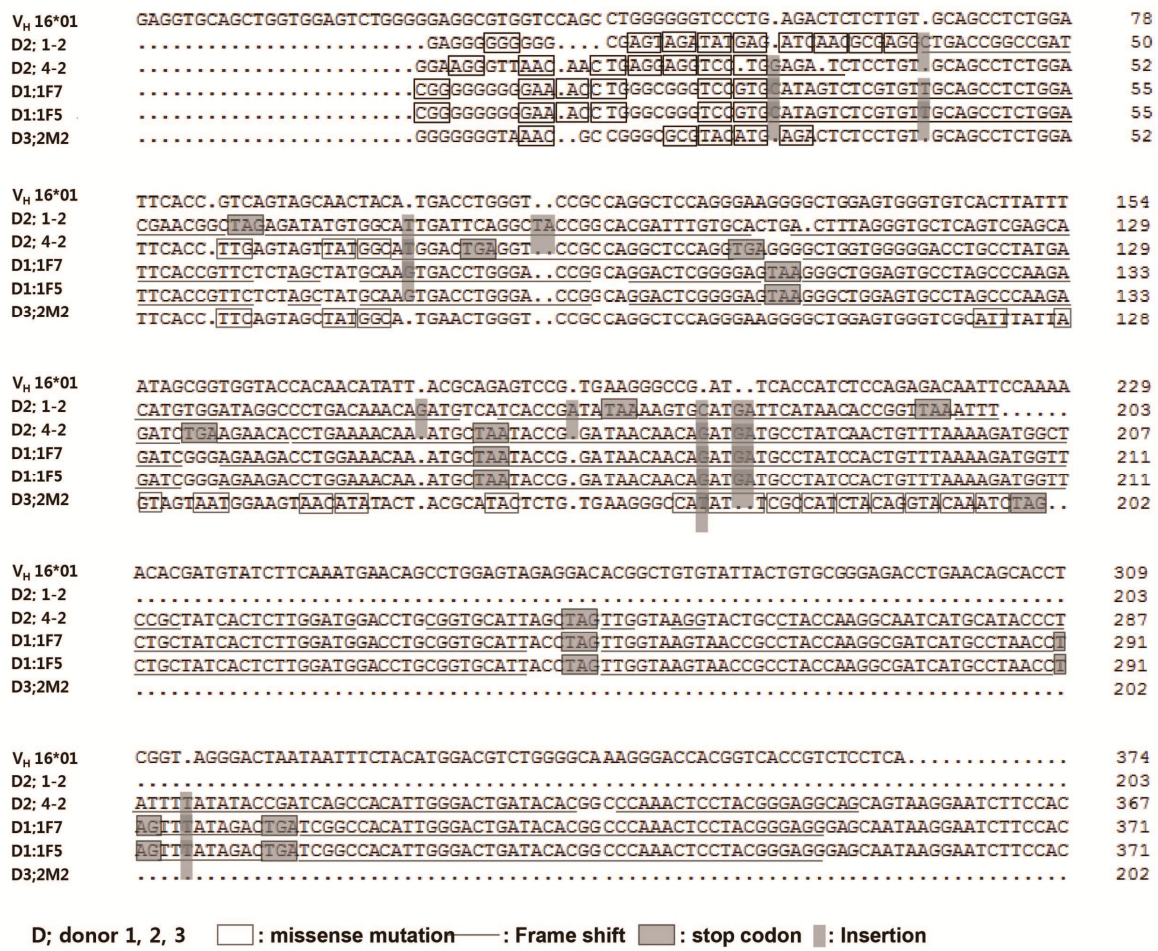

Fig. S14. Evidence of somatic hypermutations in spleen of EBV-infected humanized mice. Despite the presence of similarity between spleen DNAs derived from the same donors (germ line effect), all spleens had individually different mutation profiles, indicative of occurrence of somatic hypermutation.

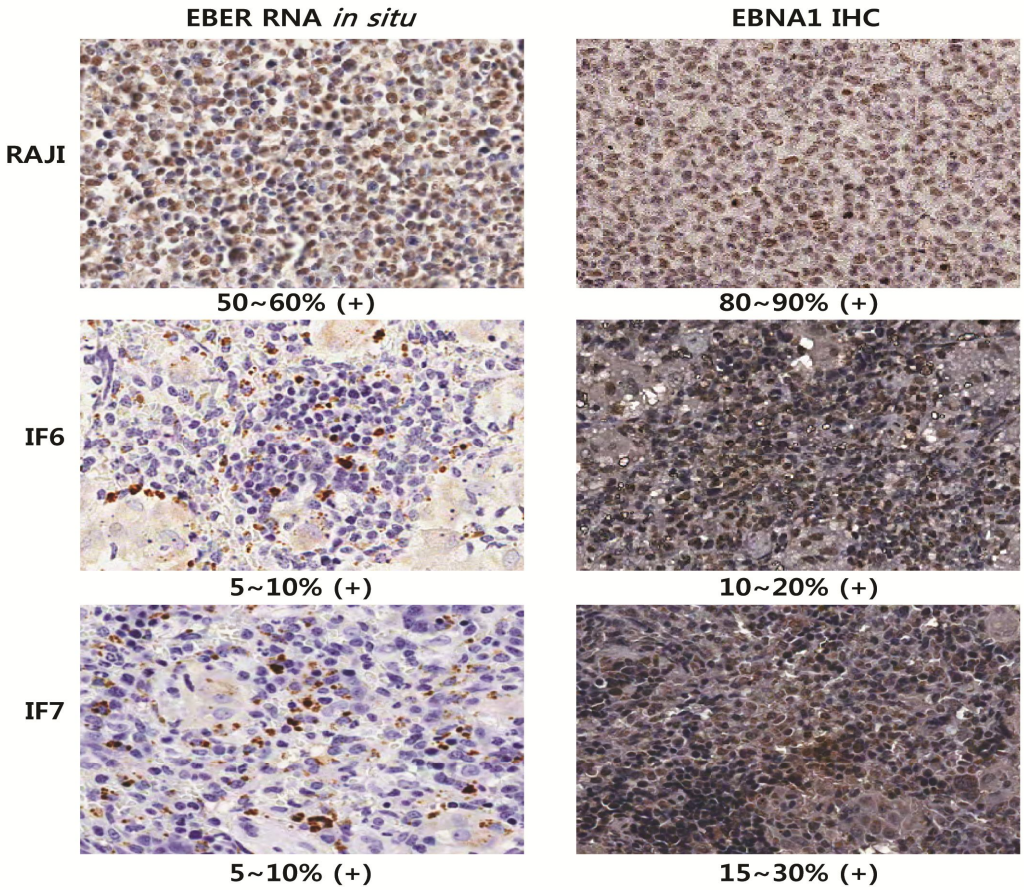

Fig. S15. Fewer number of EBER$^+$ cells than EBNA1$^+$ cells. Consecutive spleen tissue slices from EBV-infected humanized mice (IF6, IF7) and EBV-infected Burkitt's lymphoma RAJI cell line were subjected to *in situ* staining in order to compare the positive ratio of EBER- or EBNA1-expressing cells. Indicated percentage (%) denotes the proportion of positively stained cells to total cells. Note that proportion of EBER-expressing cells was smaller than that of EBNA1-expressing cells.

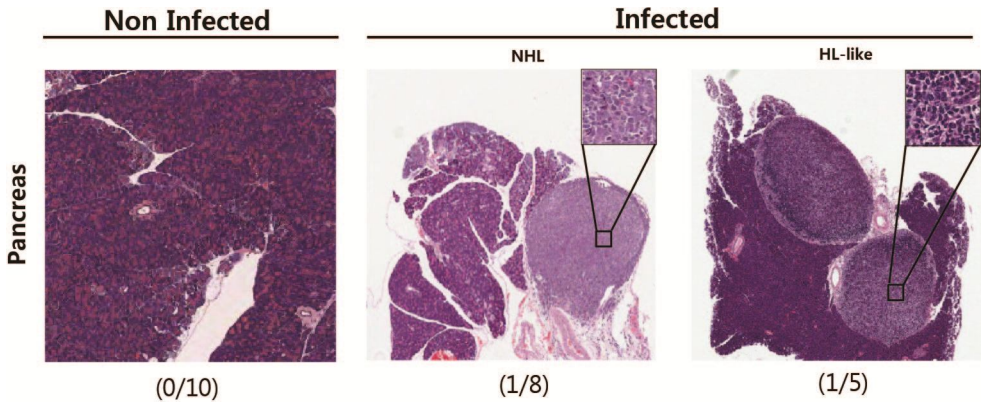

Fig. S16. Infrequent pancreatic lymphoma in EBV-infected humanized mice.

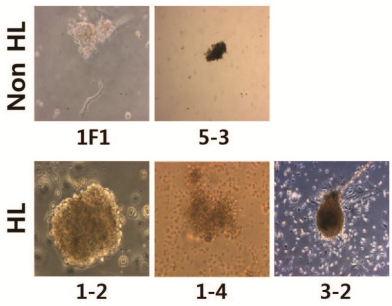

Fig. S17. *In vitro* culture of splenocytes of EBV-infected humanized mice. Though dissociated splenocytes started to grow, almost all cells stopped growing and died following 2nd~3rd passages.